Available online at www.sciencedirect.com
SCIENCE DIRECT®
International Journal of Mass Spectrometry 233 (2004) 111–116
International Journal of Mass Spectrometry
www.elsevier.com/locate/ijms

Electron impact ionization cross-sections of SF_3 and SF_5

W.M. Huo [a,*], V. Tarnovsky [b], K. Becker [b,c]

[a] NASA Ames Research Center, Mail Stop T27B-1, Moffett Field, CA 94035-1000, USA
[b] Department of Physics and Engineering Physics, Stevens Institute of Technology, Hoboken, NJ 07030, USA
[c] Center for Environmental Systems, Stevens Institute of Technology, Hoboken, NJ 07030, USA

Received 10 October 2003; accepted 3 December 2003

Abstract

We report experimental and theoretical studies of the total electron impact ionization cross-sections for the radicals SF_3 and SF_5. It is shown that for radicals with strongly polar fluoride bonds, the shielding of the attractive dipole interaction potential in the bonding region is important in a proper description of the collision process. The siBED model, which has incorporated the shielding factor, was found to provide cross-sections in agreement with recently re-analyzed experimental data for the species CF_x and NF_x ($x = 1$–3), whereas the DM model and the BEB model, on the other hand, showed large discrepancies with experiment. These findings also hold for the two free radicals SF_3 and SF_5 studied here, providing further evidence on the importance of a proper shielding of the dipole potential.

Keywords: Electron ionization; Cross-sections; Free radicals; Plasma processing

1. Introduction

Electron impact ionization plays an important role in a variety of plasma-based applications. To develop a fundamental understanding of the collision process, and to establish a reliable database for modeling the plasma, active experimental studies of electron impact ionization cross-sections are being carried out in several laboratories around the world. Reliable experimental determinations of cross-sections for ionization and dissociative ionization of molecular targets have benefited greatly from the pioneering work of Märk and co-workers [1], who were the first to recognize that the excess kinetic energy of fragment ions can cause serious errors in cross-section measurement because of discrimination effects in extracting the energetic fragment ions from the ion source and in their transport to the detector with 100% efficiency. Märk and co-workers also proposed detailed experimental checks to quantify discrimination effects, which are by now routinely performed by experimentalists who measure molecular dissociative ionization cross-sections.

Of the atoms and molecules studied experimentally, radicals pose the most challenging problems, both because of their short lifetime and their corrosive effects on the instrument. On the other hand, radicals play important roles in many plasma processes because of their reactivity and it is important to model their behavior correctly in plasma simulations. Essentially, all measurements of ionization cross-sections for free radicals were done using the fast-neutral-beam technique pioneered by Freund and co-workers [2] and subsequently used extensively by Becker and co-workers [3]. The emphasis in these measurements is on radicals important in the modeling of plasma processing in the microelectronics industry, including CH_x ($x = 1$–3) [4,5], CF_x ($x = 1$–3) [6–8], NF_x ($x = 1$–2) [8–10], and SiF_x ($x = 1$–3) [11–13]. Two additional radicals, SF_3 and SF_5, produced by the dissociation of SF_6 have also been studied using this method [14].

On the theoretical side, ab initio (e,2e) calculations for molecules are not yet feasible at present. Current theoretical studies of electron impact ionization of molecules all employ approximations derived from physically based models. The two most popular models are the binary-encounter Bethe (BEB) model of Kim and Rudd [15] and the Deutsch–Märk (DM) model of Deutsch and Märk [16]. The BEB model employs a modified form of the Mott cross-section to represent ionization by short-range interactions, and a one-term representation of the Bethe dipole cross-section with a modified energy expression to describe ionization by long-range

* Corresponding author. Fax: +1-650-604-1095.
E-mail address: whuo@mail.arc.nasa.gov (W.M. Huo).

1387-3806/$ – see front matter © 2004 Elsevier B.V. All rights reserved.
doi:10.1016/j.ijms.2003.12.011

dipole interactions. In the DM model, the Bohr radius in the semiclassical binary-encounter approximation [17] is replaced by the radius of the atomic orbital, and in the case of molecules Mulliken population analysis is used to determine the population densities of atomic orbitals in a molecule. The cross-sections determined using both models are in generally good agreement with experiment and with each other. In addition to the above two, Khare et al. [18] introduced a version of binary-encounter dipole model that also uses the Bethe cross-section to represent the long-range dipole interaction. In the CSP-ic model of Joshipura et al. [19], the total inelastic cross-section is determined using a spherical, energy-dependent complex optical potential obtained using a single-center expansion of the atomic/molecular charge densities. The total, single ionization cross-section is then deduced based on an empirical partitioning of the total inelastic cross-section into excitations to the bound and continuum states.

For a large class of atoms and molecules, the theoretical models cited above generally provide total, single ionization cross-sections that agree well with experiment. However, for a group of fluoride radicals, such as CF_x and NF_x ($x = 1$–3), the discrepancies between experiment and theory are as large as 50–100%. This rather surprising result was explained in our recent combined theoretical and experimental study [8]. It was pointed out that for this group of radicals, the strongly polar fluorine bonds pull the nonbonding electrons of the radical into the bonding region, resulting in a building up of charges there. A theoretical treatment of electron collisions with fluoride radicals must account for these bonding characteristics because the strong repulsive field in the bonding region plays an important role in electron–radical collisions when the colliding electron approaches the bonding region. The lack of an adequate description of this bonding characteristics in the theoretical models mentioned in the preceding paragraph is the source of the large discrepancy between theory and experiment. The improved binary-encounter dipole model (iBED) developed by one of us [20], and the simplified version of this model (siBED), accounts for the shielding of the long-range dipole potential by the repulsive field in the bonding region. The shielding parameter is deduced using ab initio calculations of the electric field that the molecular charge distribution exerts on the incoming electron. For CF_x and NF_x, cross-sections calculated using the siBED model are in agreement with experiment to within experimental error.

The SF_x ($x = 1$–5) radicals are produced from the parent SF_6 molecule by collisional dissociation and photodissociation. SF_6 is used widely in the electric power industry. It is also used in pulsed power generation, gas lasers, and plasma processing. Positive ion formation by electron impact of SF_6 under controlled single collision conditions have been studied by Rapp and Englander-Golden [21], who measured total ionization cross-sections, and by Stanski and Adamczyk [22] and Märk and co-workers [23], who determined partial SF_6 ionization cross-sections using two different mass spectrometric techniques. Kim and co-workers reported calculations of the total SF_6 ionization cross-section by electron impact using the BEB model [24] and Deutsch et al. [25] calculated the same quantity using the DM method. Good agreements between theory and experiment, and also between the two theoretical calculations, were obtained. Tarnovsky et al. [14] reported the first experimental measurements of the electron impact ionization cross-sections of SF_3 and SF_5. While only SF_3^+ is produced in the electron impact ionization of SF_3, they reported both the parent ion SF_5^+ as well as the fragmented product SF_3^+ in their measurements. Tarnovsky et al. also presented calculated total single ionization cross-sections for SF_x ($x = 1$–6) using an empirical modified additivity rule, MAR [26]. Good agreement between experiment and the MAR cross-sections was obtained for SF_3 and SF_5, but it should be noted that the MAR contains empirically determined fitting parameters and is thus not comparable in principle to the more rigorous DM and BEB methods. More recent calculations using the DM method led to SF_3 cross-sections up to 70% larger than experiment (H. Deutsch, M. Probst, K. Becker, T.D. Märk, personal communication, 2002). Note that both SF_3 and SF_5 are radicals with one central atom and strongly polar fluoride bonds, just like the fluorides CF_x and NF_x ($x = 1$–3) in our previous study. However, there are also differences. SF_3 and SF_5 have extravalent bonds by promotion to the 3d shell of S. Also, S is a second row atom. It is of interest to see if our model also applies to the present case.

The theoretical treatment is presented in Section 2 together with the determination of the molecular parameters. The re-analysis of the experimental data is presented in Section 3. The experimental and theoretical cross-sections are compared in Section 4.

2. Theoretical calculations

In the iBED model [20], the electron impact cross-section σ_{po}^{iBED} of ionizing an electron initially in orbital o of the target and resulting in an ion state p is given by

$$\sigma_{po}^{iBED} = \sigma_{po}^{dB} + \sigma_{po}^{BE}. \quad (1)$$

Here, σ_{po}^{dB} is the dipole Born cross-section that describes the dipole interaction between the scattering electron and the target. σ_{po}^{BE} is a modified Mott cross-section with the incident electron energy replaced by the average energy from the binary-encounter model. It accounts for both direct and exchange contributions from close collisions and is given by

$$\sigma_{po}^{BE} = \frac{4\pi N_o}{k_o^2 + \kappa_o^2 + \alpha_o^2}\left[\frac{k_o^2 - \alpha_o^2}{k_o^2\alpha_o^2} - \frac{1}{k_o^2 + \alpha_o^2}\ln\left(\frac{k_o^2}{\alpha_o^2}\right)\right], \quad (2)$$

with N_o the occupation number of orbital o, α_o^2 twice its binding energy, and κ_o and k_o the momentum of the bound electron and the incoming electron, respectively.

While the binary-encounter cross-section used in the iBED model is identical with the BED/BEB model [15] of Kim and Rudd, different dipole terms are used in the two models. In the BED/BEB model the Bethe dipole cross-section is used, representing the high-energy limit of the dipole interaction where only the long range dipole potential is important. The iBED model, on the other hand, employs a three-term polynomial derived from a series representation of the generalized oscillator strength of electron impact ionization. This representation not only describes the long-range electron-target dipole interaction, but also the shielding of the dipole field as the scattering electron comes inside the bonding region. The three-term dipole Born cross-section is given by

$$\sigma_{\mathrm{po}}^{\mathrm{dB}} = \int_0^{(k_\mathrm{o}^2-\alpha_\mathrm{o}^2)/2} \mathrm{d}E_\mathrm{p} \frac{8\pi(k_\mathrm{p}^2+\alpha_\mathrm{o}^2)^5}{k_\mathrm{o}^2} \frac{\mathrm{d}f_{\mathrm{po}}^{(\mathrm{o})}}{\mathrm{d}E_\mathrm{p}} \times \int_{K_{\min}}^{K_{\max}} \mathrm{d}K \frac{(1+d_1 t+d_2 t^2)\mathrm{d}K}{K[(K+k_\mathrm{p})^2+\alpha_\mathrm{o}^2]^3[(K-k_\mathrm{p})^2+\alpha_\mathrm{o}^2]^3}. \quad (3)$$

Here, the energy and momentum of the ejected electron is given by E_p and k_p. Also, K is the momentum transfer of the scattering electron, and $\mathrm{d}f_{\mathrm{po}}^{(0)}(E_\mathrm{p})/\mathrm{d}E_\mathrm{p}$ the optical oscillator strength (OOS) for the corresponding photoionization process. The variable t is given by

$$t = \frac{K^4}{[(K+k_\mathrm{p})^2+\alpha_\mathrm{o}^2][(K-k_\mathrm{p})^2+\alpha_\mathrm{o}^2]}. \quad (4)$$

The parameters d_1 and d_2 describe the shielding of the dipole potential.

The total single ionization cross-section of a molecule is given by

$$\sigma_{\mathrm{iBED}} = \sum_\mathrm{o}\sum_\mathrm{p} \sigma_{\mathrm{po}}^{\mathrm{iBED}}. \quad (5)$$

The data needed for the calculation of σ_{iBED} are ionization potentials, kinetic energies of the bound electrons, the OOS and the shielding parameters d_1 and d_2. In the iBED model, the OOS are either deduced from experiment or determined from ab initio calculations. In the simplified version of the iBED model (siBED), the following approximate expression is used based on the *f*-sum rule and the proper representation of the OOS in the complex k_p plane [20],

$$\frac{\mathrm{d}f_{\mathrm{po}}^{(\mathrm{o})}(E_\mathrm{p})}{\mathrm{d}E_\mathrm{p}} = \frac{8\alpha_\mathrm{o}^2 N_\mathrm{o} k_\mathrm{p}}{\pi(k_\mathrm{p}^2+\alpha_\mathrm{o}^2)^6}. \quad (6)$$

The determination of the parameters used in our siBED calculations is given separately below.

2.1. Equilibrium geometries of SF_3 and SF_5

The equilibrium geometries of the ground states of SF_3 and SF_5 were optimized using the complete active-space self-consistent field (CASSCF) method [27] and the cc-pVDZ basis of Gaussian functions [28,29]. The optimized equilibrium geometry for the ground state of SF_3 is umbrella shape with S at the top and the three F atoms at the bottom. The bond lengths of two of the S–F bonds are 3.21 bohr and the bond length of the slightly shorter S–F bond is 3.08 bohr. The bond angle between the two longer S–F bonds is 154.75° and the two other F–S–F bond angles are 87.90°. This geometry is different from the geometry tabulated in JANAF tables [30] with three equal S–F bonds at 2.95 bohr and all F–S–F bond angle at 109.47°. The ground state energy calculated using the couple-cluster singles and doubles with perturbation treatment of triples (RCCSD(T)) method [31,32] at the optimized geometry is 0.07793 hartree lower than the energy at JANAF geometry. Also, the first ionization potential (IP) determined using the optimized geometry is 11.26 eV, in close agreement with the 11.36 eV determined from the experiment of Tarnovsky et al. [14]. In comparison, the first IP determined using JANAF geometry is 6.97 eV. Based on this comparison, the optimized geometry is used in our siBED cross-section calculations for SF_3.

The optimized geometry of SF_5 is the same as listed in JANAF tables. SF_5 is pyramidal, with S in the center of the square formed by four F atoms and the fifth F at the top of the pyramid. The bond length of an in-plane S–F bond is 2.986 bohr, and the bond length of the out-of-plane S–F bond is 2.853 bohr.

2.2. Binding energies and kinetic energies

The binding energies, $-\alpha_\mathrm{o}^2/2$, and kinetic energies, $\kappa_\mathrm{o}^2/2$, of molecular electrons were determined using quantum chemistry calculations. It has been shown previously that for molecules containing atoms from the second row or higher, the use of a quasi-relativistic effective core potential to represent the core electrons eliminates the problem of large bound-electron kinetic energies resulting from the strong attractive potential from the high-*Z* nucleus [33]. Thus, our calculations employed the 10-electron quasi-relativistic effective core potential derived by the Stuttgart group for sulfur [34]. The kinetic energies of the molecular electrons were calculated using Hartree–Fock functions because one-electron properties calculated using Hartree–Fock calculations were variationally stable to the first order. The binding energies for valence electrons were calculated as the difference between the energies of the ion and the neutral molecule. For the lowest ion state of each geometry, the RCCSD(T) method was used for the calculation. For the higher lying ion states the CASSCF method was employed and the result was scaled by the difference between the CASSCF and RCCSD(T) result for the lowest state. For the inner electrons SCF values based on Koopmans theorem were used. Also, for inner electrons with less than 1 hartee binding energy, the Koopmans values are scaled by the CASSCF corrections determined for valence electrons.

Table 1
Binding energies ($-\alpha_o^2/2$) and kinetic energies ($\kappa_o^2/2$) used in the siBED calculations of SF_3 and SF_5

SF_3 (X^2A')[a]			SF_5 (X^2A_1)[b]		
Orbital	$-\alpha_o^2/2$	$\kappa_o^2/2$	Orbital	$-\alpha_o^2/2$	$\kappa_o^2/2$
7a′	45.908[c]	93.702	$7a_1$	49.228[c]	79.166
8a′	43.454[c]	104.508	$8a_1$	45.685[c]	104.622
9a′	25.448[d]	47.423	$9a_1$	44.439[c]	109.839
10a′	18.389[d]	66.038	$10a_1$	27.040[d]	68.581
11a′	18.079[d]	75.041	$11a_1$	21.511[d]	71.349
12a′	15.846[e]	83.162	$12a_1$	17.369[d]	87.239
13a′	14.422[e]	86.968	$13a_1$	17.337[e]	86.710
14a′	13.300[f]	64.239	$14a_1$	16.394[f]	89.007
15a′	11.263[f]	43.063	$15a_1$	11.573[f]	55.055
3a″	43.560[c]	102.150	$3b_1$	45.786[c]	99.410
4a″	19.255[d]	70.756	$4b_1$	21.685[d]	71.218
5a″	17.207[e]	79.441	$5b_1$	18.711[d]	78.909
6a″	15.175[e]	82.896	$6b_1$	16.390[e]	89.297
7a″	15.006[f]	91.449	$7b_1$	16.040[f]	94.628
			$3b_2$	45.786[c]	99.410
			$4b_2$	21.685[d]	71.218
			$5b_2$	18.711[d]	78.909
			$6b_2$	16.390[e]	89.297
			$7b_2$	16.040[f]	94.628
			$1a_2$	18.915[e]	75.514
			$2a_2$	15.267[f]	97.210

Core electrons are not listed. Both quantities are in eV.
[a] SF_3 calculations were done using C_s symmetry.
[b] SF_5 calculations were done using C_{2v} symmetry.
[c] Hartree–Fock calculation based on Koopman's theorem.
[d] Scaled Hartree–Fock calculation.
[e] CASSCF calculation corrected by RCCSD(T) results.
[f] RCCSD(T) calculation.

The aug-cc-pVTZ basis of Gaussian functions was used in the SF_3 calculations whereas for SF_5 the cc-pVTZ basis was used. All calculations employed the MOLPRO electron structure code [35]. Table 1 presents the binding energies and kinetic energies for SF_3 and SF_5. Since our calculations used a 10-electron effective core potential, sulfur 1s, 2s, and 2p electrons are not included in the tabulation. The data on fluoride 1s electrons are also skipped because their energies are too high to play a role in the range of electron energies studied here.

2.3. Shielding parameters d_1 and d_2

The parameters d_1 and d_2 in Eq. (3) represent the shielding the attractive long-range dipole potential as the scattering electron approaches the bonding region. In our study of CF_x and NF_x, the parameter d_1 was determined by comparison of the molecular property F of the radical with the corresponding value for a non-fluoride molecule at the same geometry. The property F is given by

$$F = \sum_i \sum_\mu (f_{e\mu}^i)^2, \tag{7}$$

with $f_{e\mu}^i$ the electric field exerted by the molecular charge distribution of orbital i on an electron. At the equilibrium geometry of SF_3, the value of F for SF_3 is 0.5079 versus a value of 0.4448 for CF_3 at the same geometry. Based on the ratio of the two F values and the previously determined $d_1 = -4.8$ for CF_3, we set $d_1 = -5.5$ for SF_3.

Due to the use of the effective core potential in the calculation of molecular parameters, the region near the sulfur nucleus is described differently from all-electron calculations. The parameter d_2, which describes the interaction of the scattering electron with the inner region of the molecular charge distribution, is chosen to be 1.2 for SF_3 to reflect the less repulsive core region.

For SF_5, there are no corresponding AB_5 molecules to guide the choice of d_1 and d_2. Instead, we consider the bonding trend in the series of SF_x molecules. While all SF_x (x = 3–6) has extravalent bonds, SF_6 is a closed shell molecule for which the BEB cross-sections are in good agreement with experiment [24]. Thus, the bonding characteristics changes from $x = 3$ to 6. Based on this consideration, the parameters d_1 and d_2 for SF_5 are chosen to be 3/5 of the values of SF_3.

3. Analysis of experimental data

We carefully re-analyzed the originally reported experimental cross-section data for SF_3 and SF_5 [14], an effort to ensure that systematic effects that may influence the proper determination of the total single ionization cross-sections are fully accounted for to the maximum extent possible. The total single ionization cross-section for each free radical is obtained as the sum of all measured partial ionization cross-sections. The sum of all partial ionization cross-sections for a given target will only yield the "correct" total single ionization cross-section, if all channels leading to the formation of one singly charged positive ion are properly taken into account. This requires estimates for contributions to the total single ionization cross-section from partial ionization channels whose cross-sections were not or not accurately measured because of weak signals and/or significant excess kinetic energy that precludes a 100% collection of a specific fragment ion. Another issue is the presence of (positive) ion–(positive) ion pair formation processes whose contributions to the total single ionization cross-section have to be discounted which requires that their respective absolute cross-sections and energy dependences have to be determined or estimated. In the course of the present work, we re-analyzed all original data files relating to the measurements of the SF_3 and SF_5 partial ionization cross-sections in an effort to obtain the most reliable experimental total single electron impact ionization cross-sections for these two free radicals. The re-analysis of the data sets resulted in SF_3 and SF_5 cross-sections that were at most 3% different (in the low-energy regime from threshold to 100 eV) from those published earlier [14]. This change is much smaller that the overall error margins for the experimentally determined total SF_3 and SF_5 electron impact ionization cross-sections, which are of the order of ±20%.

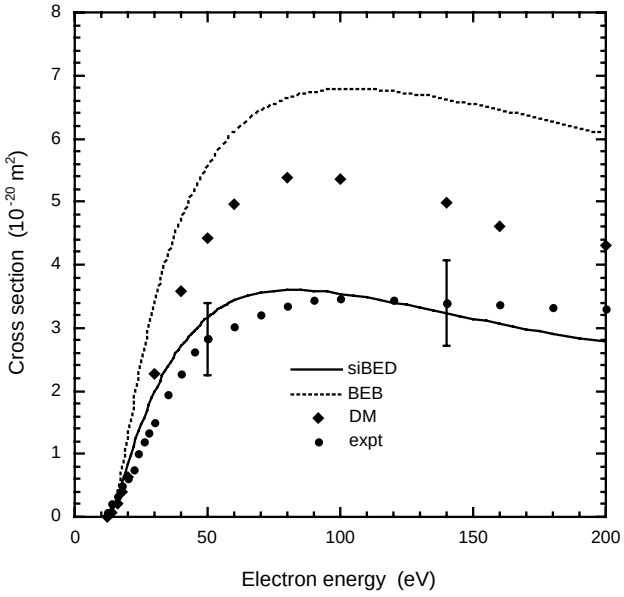

Fig. 1. Total single ionization cross-section of SF_3 calculated using the siBED model and the revised experimental data. Also presented are theoretical cross-sections calculated using the BEB model of Kim and Rudd [15] and the DM model [16].

4. Results and discussions

Figs. 1 and 2 present the total single ionization cross-sections of SF_3 and SF_5, respectively, calculated using the siBED model and the re-analyzed experimental data. Also presented are the DM cross-sections (H. Deutsch, M. Probst, K. Becker, T.D. Märk, personal communication, 2002) and the BEB cross-sections calculated using the molecular data from Table 1. For both SF_3 and SF_5, good agreement is obtained between experiment and the siBED cross-sections, to within experimental error. While the siBED cross-section curve for SF_5 follows the shape of the experimental curve well, the siBED curve for SF_3 at the high-energy end decreases with energy somewhat faster than experiment.

Comparison of experiment with the DM and BEB data shows that, for both SF_3 and SF_5, these two models give cross-sections that are larger than experiment. But the deviation between DM model and experiment is generally smaller than the BEB model. For SF_5 the DM cross-sections are within experimental error of our measurement, even though they are somewhat higher than the siBED result. This probably is related to our observation that the bonding characteristic of SF_5 is closer to normal bonding than SF_3.

The present study shows that the siBED model, which accounts for the shielding of the dipole interaction, is capable to describe electron impact ionization of radicals with extravalent bonding.

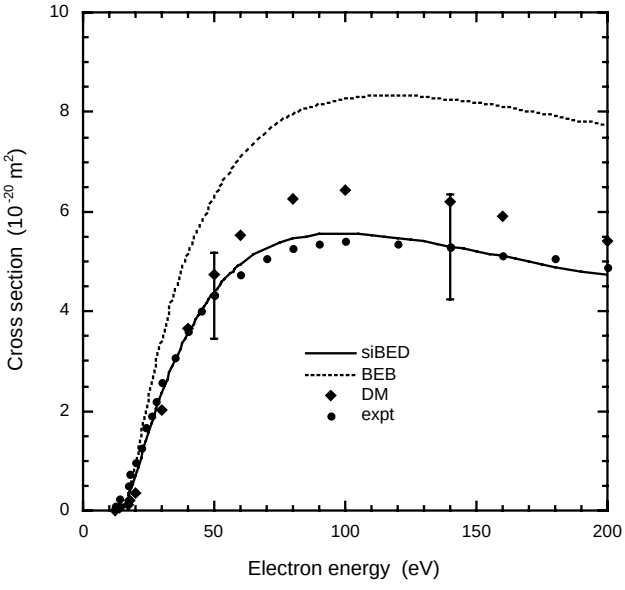

Fig. 2. Total single ionization cross-section of SF_5 calculated using the siBED model and the revised experimental data. Also presented are theoretical cross-sections calculated using the BEB model of Kim and Rudd [15] and the DM model [16].

Acknowledgements

The authors acknowledge helpful discussion with H. Deutsch, M. Probst, and T.D. Märk as well as their willingness to make available unpublished data of DM calculations for the two targets studied here. Two of us (V.T., K.B.) would like to acknowledge partial financial support from the Division of Chemical Sciences, Office of Basic Energy Sciences, Office of Science, U.S. Department of Energy.

References

[1] H.U. Poll, C. Winkler, D. Margreiter, V. Grill, T.D. Märk, Int. J. Mass Spectrom. Ion Processes 112 (1992) 1.
[2] F.A. Biaocchi, R.C. Wetzel, R.S. Freund, Phys. Rev. Lett. 53 (1984) 771.
[3] V. Tarnovsky, H. Deutsch, K.E. Martus, K. Becker, J. Chem. Phys. 109 (1998) 6596, and references therein to earlier work.
[4] F.A. Baiocchi, R.C. Wetzel, R.S. Freud, Phys. Rev. Lett. 53 (1984) 771.
[5] V. Tarnovsky, A. Levin, H. Deutsch, K. Becker, J. Phys. B 29 (1996) 139.
[6] V. Tarnovsky, K. Becker, JU Chem. Phys. 98 (1993) 7686.
[7] V. Tarnovsky, P. Kurunczi, D. Rogozhnikov, K. Becker, Int. J. Mass Spectrom. Ion Processes 128 (1993) 181.
[8] W.M. Huo, V. Tarnovsky, K.H. Becker, Chem. Phys. Lett. 358 (2002) 328.
[9] V. Tarnovsky, A. Levin, K. Becker, R. Basner, M. Schmidt, Int. J. Mass Spectrom. Ion Processes 133 (1994) 175.
[10] V. Tarnovsky, A. Levin, K. Becker, J. Chem. Phys. 100 (1994) 5626.
[11] T.R. Hayes, R.C. Wetzel, F.A. Baiocchi, R.S. Freund, J. Chem. Phys. 88 (1989) 823.
[12] T.R. Hayes, R.J. Shul, F.A. Baiocchi, R.C. Wetzel, R.S. Freund, J. Chem. Phys. 89 (1989) 4035.
[13] R.J. Shul, T.R. Hayes, R.C. Wetzel, F.A. Baiocchi, R.S. Freund, J. Chem. Phys. 89 (1989) 4042.

[14] V. Tarnovsky, H. Deutsch, K.E. Martus, K. Becker, J. Chem. Phys. 109 (1998) 6596.
[15] Y.-K. Kim, M.E. Rudd, Phys. Rev. A 50 (1994) 3954.
[16] H. Deutsch, K. Becker, S. Matt, T.D. Märk, Int. J. Mass Spectrom. 197 (2000) 37.
[17] M. Gryzinski, Phys. Rev. A 138 (1965) 305.
[18] S.P. Khare, M.K. Sharma, S. Tomar, J. Phys. B 32 (1999) 3147.
[19] K.N. Joshipura, B.K. Antony, M. Vinodkumar, J. Phys. B 35 (2002) 4211.
[20] W.M. Huo, Phys. Rev A 64 (2001) 042719.
[21] D. Rapp, P. Englander-Golden, J. Chem. Phys. 43 (1965) 1464.
[22] T. Stanski, B. Adamczyk, Int. J. Mass Spectrom. Ion Processes 46 (1983) 31.
[23] D. Margreiter, G. Walder, H. Deutsch, H.U. Poll, C. Winkler, K. Stephan, T.D. Märk, Int. J. Mass Spectrom. Ion Processes 100 (1990) 143.
[24] W. Hwang, Y.-K. Kim, M.E. Rudd, J. Chem. Phys. 104 (1996) 2956.
[25] H. Deutsch, K. Becker, T.D. Märk, Int. J. Mass Spectrom. Ion Processes 167/168 (1997) 503.
[26] H. Deutsch, K. Becker, R. Basner, M. Schmidt, T.D. Märk, J. Phys. Chem. 102 (1998) 8819.
[27] The geometry optimization was done using *DALTON*. *DALTON* is a molecular electronic structure program, Release 1.2(2001), written by T. Helgaker, H.J. Aa. Jensen, P. Jørgensen, J. Olsen, K. Ruud, H. Ågren, A.A. Auer, K.L. Bak, V. Bakken, O. Christiansen, S. Coriani, P. Dahle, E.K. Dalskov, T. Enevoldsen, B. Fernandez, C. Hättig, K. Hald, A. Halkier, H. Heiberg, H. Hettema, D. Jonsson, S. Kirpekar, R. Kobayashi, H. Koch, K.V. Mikkelsen, P. Norman, M.J. Packer, T.B. Pedersen, T.A. Ruden, A. Sanchez, T. Saue, S.P.A. Sauer, B. Schimmelpfenning, K.O. Sylvester-Hvid, P.R. Taylor, and O. Vahtras.
[28] T.H. Dunning, J. Chem. Phys. 90 (1989) 1007.
[29] R.A. Kendall, T.H. Dunning, R.J. Harrison, J. Chem. Phys. 96 (1992) 6796.
[30] M.W. Chase Jr. (Ed.), NIST-JANAF Thermochemical Tables, 1998.
[31] P.J. Knowles, C. Hampel, H.-J. Werner, J. Chem. Phys. 99 (1993) 5219.
[32] J.D. Watts, J. Gauss, R.J. Bartlett, J. Chem. Phys. 98 (1993) 8718.
[33] W.M. Huo, Y.-K. Kim, Chem. Phys. Lett. 110 (1999) 3811.
[34] A. Bergner, M. Dolg, W. Kuechle, H. Stoll, H. Preuss, Mol. Phys. 80 (1993) 1431.
[35] MOLPRO is a package of ab initio program written by H.-J. Werner and P.J. Knowles with contributions from R.D. Amos, A. Bernhardsson, A. Berning, P. Celani, D.L. Cooper, M.J.O. Deegan, A.J. Dobbyn, F. Eckert, C. Hampel, G. Hetzer, T. Korona, R. Lindh, A.W. Lloyd, S.J. McNicholas, F.R. Manby, W. Meyer, M.E. Mura, A. Nicklass, P. Palmieri, R. Pitzer, G. Rauhut, M. Schütz, H. Stoll, A.J. Stone, R. Tarroni, and T. Thorsteinsson.